Syn and Anti Bent Hydrazine Radical Cations. Effect of σ,π Mixing on Spectral Properties

Stephen F. Nelsen,* Silas C. Blackstock, Nathan P. Yumibe, Timothy B. Frigo, John E. Carpenter, and Frank Weinhold

Contribution from the Department of Chemistry, University of Wisconsin, Madison, Wisconsin 53706. *Received April 13, 1984*

Abstract: Nitrogen ESR splitting constants, a(N), and π,π^* optical absorption spectrum maxima, λ_m, are compared for 15 examples of $R_4N_2^+$. Molecular orbital calculations of these quantities are compared for $H_4N_2^+$ bent anti and syn at the nitrogens. The different symmetries for syn and anti σ,π mixing cause surprisingly large differences in spectral properties depending on the type of bending at nitrogen for $R_4N_2^+$.

Tetraalkylhydrazine radical cations ($R_4N_2^+$) prefer roughly olefin-like geometries,[1] with coplanar p-rich lone pair orbitals forming a "three-electron bond" (there are two π, one π^* electrons occupying the two lone pair combination MO's). In this work the effects of pyramidalization at nitrogen on the spectroscopic properties of $R_4N_2^+$ are considered. Pyramidalization mixes s character into the lone-pair orbitals, which causes an increase in the nitrogen ESR splitting constant, a(N). Because rapid tumbling averages out the p components of the nitrogen hyperfine tensor, the isotropic a(N) value depends only on the s-orbital spin density at nitrogen. It was previously pointed out that the large range of observed $a(N)$ values of 11.5 to 28 G[2-4] can only be reasonably explained by a substantial range in the amount of pyramidality at nitrogen when the R groups of $R_4N_2^+$ are changed. In this work the $\pi\pi^*$ absorption maxima λ_m are determined for several examples of $R_4N_2^+$ and compared with their a(N) values. Bending at nitrogen will decrease lone pair, lone pair overlap, which is expected to lower the π,π^* energy gap and increase λ_m. λ_m proves to be remarkably sensitive to bending at nitrogen and to provide information on the details of the geometry changes which accompany R group changes in $R_4N_2^+$.

Results

Although a(N) values have been reported for a variety of $R_4N_2^+$,[2-4] absorption data were only reported for PF_6^- salts of the isolably stable "Bredt's rule protected" hydrazines **1**,[5] **2**,[6] and **3**.[7]

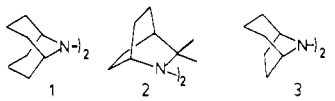

1 2 3

Since λ_m depends on solvent,[5] we consider only data in acetonitrile here. There is more than one absorption maximum for some $R_4N_2^+$ examples. As discussed elsewhere[5b] $\mathbf{1}^+\mathbf{PF}_6^-$ shows a short wavelength shoulder on the π,π^* absorption maximum at 340 nm, which we attributed to an internal charge-transfer band (σ combination orbital to π^* transition). The UV spectrum of a fourth isolable $R_4N_2^+$ example, that from **4**, is even more complex.

4

$\mathbf{4}^+\mathbf{PF}_6^-$ shows λ_m (in nm) (ϵ) values of 266 (1760), 244 (1730), 218 (1830), the BF_4^- salt 264 (1580), 243 (1520), and the NO_3^- salt 266 (1500), 200 (9400), all in acetonitrile. Both the position and the intensity of the short wavelength bonds depend strongly upon counterion, and at least one of these bands appears to involve charge transfer between the ions. Nevertheless, the long-wavelength band at 264–266 nm, which we attribute to π,π^* absorption, is insensitive to counterion.

Table I. $\pi\pi^*$ Absorption Maxima and Nitrogen ESR Splittings for Some Tetraalkylhydrazine Radical Cations

hydrazine	cation generation[a]	λ_m (ϵ)[b]	a(N)[c]
1	A	340 (4000)	13.15
2	A	303 (4500)	13.5
3	A	334 (2100)	13.7
4	A	266 (1500)	15.1[d]
5	B	283 (>1300)	16.1[d]
6	B	281 (>1100)	17.6
7	B	321 (>700)	20.95[d]
8	B	303 (>660)	13.4
9	C	289 (>1350)	13.0
10	C	286 (>900)	13.1[d]
11	C	331 (>1320)	13.1[e]
12	C	414 (>950)	11.9
13	C	266 (>1500)	13.9
14	C	260 (>1300)	16.0
15	C	270 (>1320)	15.0

[a] A, isolated as a pure solid. B, $AgNO_3$ oxidation in CH_3CN. C, electrochemical oxidation in acetonitrile containing 0.1 M n-Bu_4N^+-ClO_4^- as supporting electrolyte. [b] Solvent: acetonitrile. [c] From ref 2 unless otherwise noted. [d] Measured in this work. [e] The nitrogen splittings have not been measured accurately and probably differ at the two nitrogens.

To get a wider range of $R_4N_2^+$ examples, we wanted to include compounds which are not isolably stable. We first explored using $AgNO_3$ as oxidant, centrifuging off the silver sludge produced, and running the UV spectrum on the clear solution obtained (method B of Table I, used for compounds **5–8**). This only works

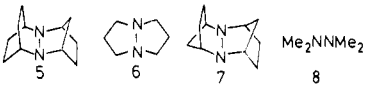

5 6 7 8

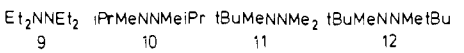

9 10 11 12

well for compounds which are easier to oxidize than tetramethylhydrazine; the oxidation is too slow otherwise. A second problem is that $AgNO_3$ absorbs strongly below about 260 nm, which interferes with the π,π^* band we wish to observe in some cases. We therefore switched to an electrochemical oxidation method (method C). A 1–2 mM solution of the hydrazine in acetonitrile containing 0.1 M n-Bu_4NClO_4 as supporting electrolyte is forced by syringe pump through reticulated vitreous carbon maintained at a high enough potential to oxidize the hydrazine and through a flow UV cell. For most $R_4N_2^+$ examples, the flow (and current) may be stopped and the UV spectrum of the cation radical recorded at leisure, since millimolar solutions of most $R_4N_2^+$ examples are stable for hours at room temperature. This

(1) Nelsen, S. F. *Acc. Chem. Res.* **1981**, *14*, 131.
(2) Nelsen, S. F.; Weisman, G. R.; Hintz, P. J.; Olp, D.; Fahey, M. R. *J. Am. Chem. Soc.* **1974**, *96*, 2196.
(3) Nelsen, S. F.; Echegoyen, L. *J. Am. Chem. Soc.* **1975**, *97*, 4930.
(4) Nelsen, S. F.; Kessel, C. R.; Brace, H. W. *J. Am. Chem. Soc.* **1979**, *101*, 1874.
(5) (a) Nelsen and Kessel report λ_m = 345 nm in 95% ethanol: Nelsen, S. F.; Kessel, C. R. *J. Am. Chem. Soc.* **1977**, *99*, 2392. (b) Nelsen et al. report λ_m = 340 nm in acetonitrile, the solvent used throughout this work: Nelsen, S. F.; Teasley, M. F.; Kapp, D. L.; Kessel, C. R.; Grezzo, L. A. *J. Am. Chem. Soc.* **1984**, *106*, 791.
(6) Nelsen, S. F.; Gannett, P. M. *J. Am. Chem. Soc.* **1982**, *104*, 5292.
(7) Nelsen, S. F.; Cunkle, G. T.; Evans, D. H. *J. Am. Chem. Soc.* **1983**, *105*, 5928.

0002-7863/85/1507-0143$01.50/0

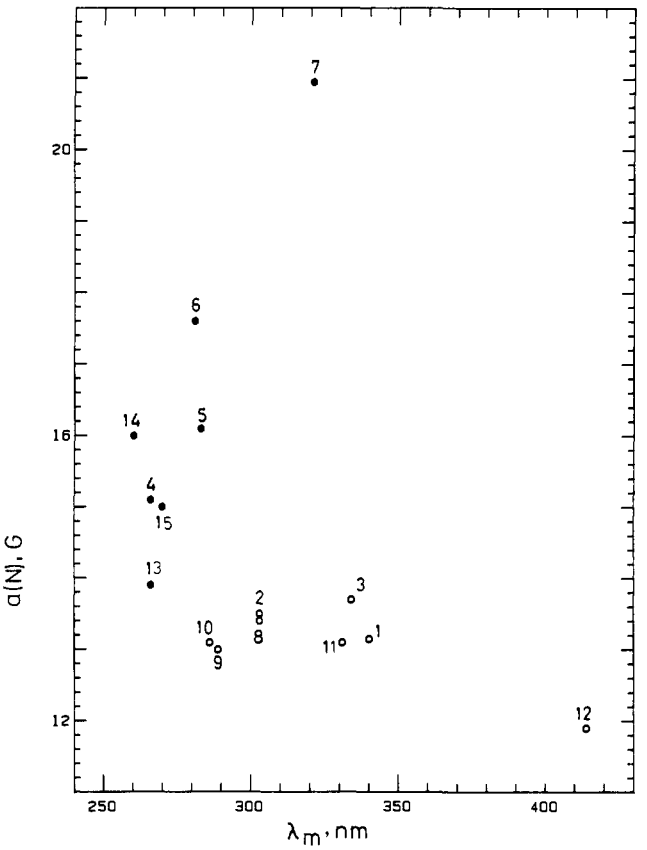

Figure 1. Plot of a(N) vs. λ_m for some tetraalkylhydrazines.

allows λ_m measurement to be made easily on most examples of $R_4N_2^+$ and only requires a few milligrams of hydrazine. The minimum ϵ values quoted were calculated by assuming 100% yield of $R_4N_2^+$. Method C was used for acyclic hydrazines **9–12** and cyclic hydrazines **13–15**.

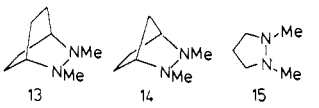

13 14 15

Table I contains a(N) and λ_m data for 15 examples of $R_4N_2^+$, which are plotted in Figure 1. Two types of symbols are used in the plot to emphasize the effect of alkyl group structure on these spectroscopic data. The *N,N*-bicycloalkyl and acyclic examples (**1–3** and **8–12**, respectively) are shown with open circles and show a distribution with a small range in a(N) but wide variation in λ_m, so they exhibit a low $a(N)/\lambda_m$ slope. In contrast, the *N,N'*-cycloalkyl compounds **4–7** and **13–15** (shown as filled circles) exhibit a much larger $a(N)/\lambda_m$ slope. We argue that these distributions correspond to anti and syn bent $R_4N_2^+$, respectively.

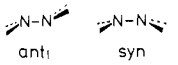

Anti bending is preferred on both steric and electronic grounds (see below), and its has been shown that crystalline 3^+ is anti bent by X-ray crystallography.[8] We feel it is clear that the open circles correspond to anti bent $R_4N_2^+$ structures. On the other hand, the bis(*N,N'*-cycloalkyl) examples **4–7** are forced into syn bent geometries by rings holding both CNNC dihedral angles near 0°. Even their neutral forms are forced to assume conformations with lone pair,lone pair dihedral angle θ near 0°, despite the electronic preference for θ to be near 90° when there are four lone pair electrons.[1] Examples **13–15** have only one CNNC angle restricted to be small, but they clearly fall in the syn distribution on the a(N) vs. λ_m plot, not the anti one. We suggest syn geometries occur

(8) Manuscript in preparation.

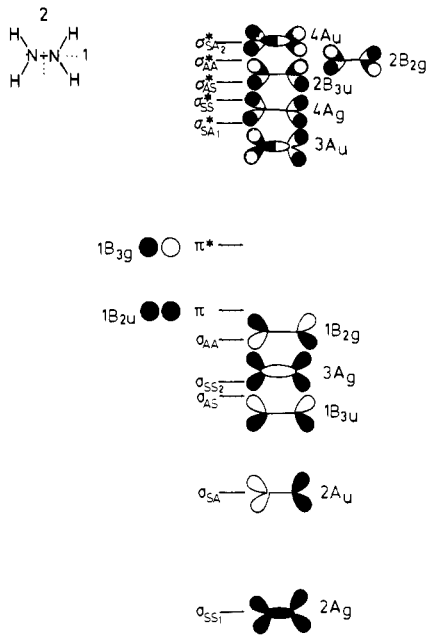

Figure 2. Stylized representations of the MO's for planar H_4N_2. The energies plotted are calculated for H_4N_2 in the geometry of the MNDO energy minimized planar $H_4N_2^+$.

Scheme I

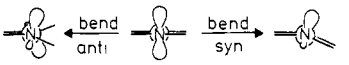

for these $R_4N_2^+$ examples because of the restoring force for coplanar lone pair orbitals in three-electron π bonds. If one CNNC angle is held near 0° and the nitrogens bend anti, the lone pair orbitals axes are forced out of coplanarity, as indicated in Scheme I. *Syn* bending, on the other hand, keeps the lone pair axes in the electronically stabler coplanar orientation. Twisting the lone pair orbital axes all the way to 90° in 3^+ has been shown to cost over 21 kcal/mol in energy.[7]

Figure 1 suggests, then, that the π,π^* transition energy, which is experimentally measured by λ_m, is quite sensitive to the difference in bending in anti and syn directions, as is the nitrogen splitting observed. To understand why the $R_4N_2^+$ system shows such large changes in these spectral parameters, we will consider orbital mixing in the parent system, $H_4N_2^+$.

σ,π Mixing in Hydrazine Radical Cation. Planar $H_4N_2^+$ has two lone pair orbitals and five σ bonds. The four NH bonds form bonding MO's of SS, SA, AS, and SS symmetry with respect to planes 1 and 2 (parallel to the NN bond perpendicular to the molecular plane, and bisecting the NN bond) which appear as lines 1 and 2 in the view of the molecule from the top, Figure 2. The NN bond mixes with the SS NH combination orbital in bonding (σ_{SS1}) and anti bonding (σ_{SS2}) combinations. Analogous σ antibonding orbital combinations occur. Neither σ nor σ^* orbitals, which are symmetric with respect to the molecular plane, can mix with π or π^*, which are antisymmetric with respect to the molecular plane. Figure 2 shows a stylized pictorial representation of these orbitals, along with their D_{2h} symmetry labels (from Jorgenson and Salem's representation of ethylene,[9] which is isoelectronic with $H_4N_2^{2+}$).

Bending at nitrogen allows σ,π mixing. As Vollard, Davidson, and Borden pointed out for ethylene,[10] bending syn and anti causes different σ and σ^* orbitals to mix with π and π^*. The orbitals that are antisymmetric with respect to plane 1 of Figure 2 are unable to mix with the π orbitals, which always are S with respect to plane 1. Plane 2 no longer properly describes the symmetry

(9) Jorgensen, W. L.; Salem, L. "The Organic Chemist's Book of Orbitals"; Academic Press: New York, 1973; p 81.

(10) Vollard, W. V.; Davidson, E. R.; Borden, W. T. *J. Am. Chem. Soc.* **1979**, *101*, 533.

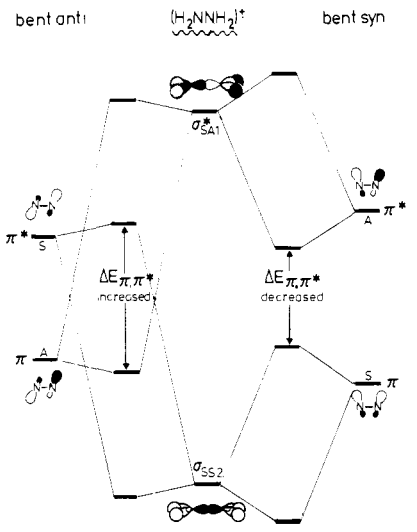

Figure 3. Qualitative plot showing mixing of the σ HOMO and σ^* LUMO of $H_4N_2^+$ with the π and π^* levels for anti and syn bending at the nitrogens.

when the nitrogens bend because although the syn bend compound retains 2 as a symmetry plane, the anti bent compound has a C_2 axis bisecting the NN bond, not a plane of symmetry. Nevertheless, inspection of Figures 2 and 3 will show that the S plane 1 orbitals which are S plane 2 in Figure 2 have the proper symmetry to mix with π upon bending syn and with π^* upon bending anti, while the S plane 1 and A plane 2 orbitals have the opposite behavior, mixing with π^* in the syn bend and with π in the *anti* bend compound. Because orbital mixing is inversely proportional to their energy gap when overlap is similar,[11] the most important σ orbitals for mixing with the π orbitals are $\sigma_{SA1}{}^*$ and σ_{SS2}, which are redrawn in side view at the center of Figure 3. The π and π^* orbitals for anti and syn bent $H_4N_2^+$ are shown at the left and right of Figure 3, respectively. Bending anti mixes σ_{SS2} with π^* and the σ^* LUMO with π, while bending syn mixes σ_{SS2} with π and the σ^* LUMO with π^*. There is greater σ,π mixing for a given amount of bend syn than for the same amount of bend anti, because the energy gap between the mixing orbitals is smaller. As for ethylene,[10] anti bending is preferred (stabilization of the doubly occupied π orbital is energetically more important than destabilization of the singly occupied π^* orbital). MO calculations at various levels (INDO, MNDO, STO-3G) predict anti bent $H_4N_2^+$ to be stabler than syn bent, and both are stabler than the planar form. The energy differences are small, and 6-31G calculations get the planar form as the stablest one (see Below). Bending at the nitrogens is calculated to be quite easy by all methods.

We shall use α_{av} (the average of the two NNH and the HNH bond angles) as our measure of the amount of bending at nitrogen, for reasons previously discussed.[12] It has been previously pointed out that bending syn increases a(N) more than bending anti.[2,13] Figure 3 makes the reason clear; σ,π mixing is larger for syn bending because of a substantially smaller energy gap, so the syn π orbitals get more s character.

Molecular Orbital Calculations on $H_4N_2^+$. We have carried out molecular orbital calculations on $H_4N_2^+$ which is forced to bend in syn and anti directions to see how the qualitative orbital mixing discussed above would actually be expressed in the spectroscopic properties of hydrazine radical cations. Unrestricted Hartree–Fock calculations were done by using Dewar's semiempirical MNDO method[14] and ab initio calculations at the STO-3G and 6-31G levels by using Pople's GAUSSIAN 77 package.[15]

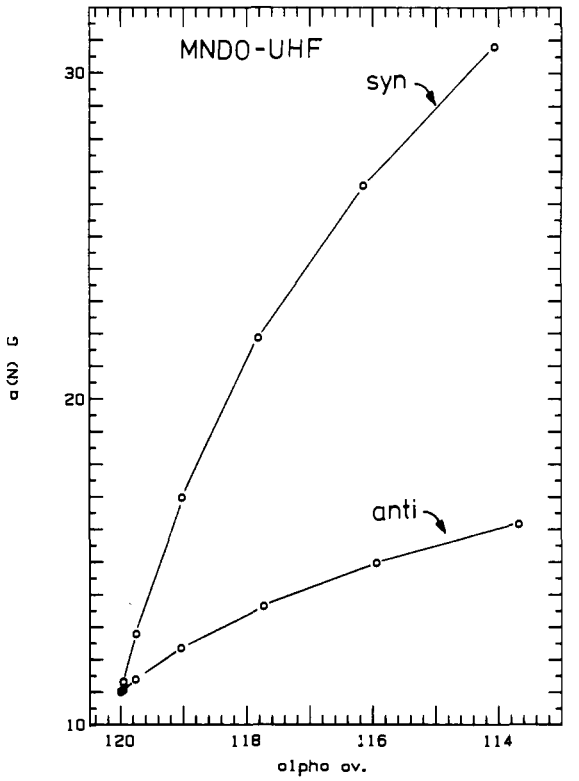

Figure 4. Plot of a(N) vs. α_{av} for $H_4N_2^+$ as calculated by the MNDO–UHF method.

A plot of MNDO-calculated a(N) vs. α_{av} appears as Figure 4. We used Pople's INDO-derived proportionality constant of 379.34 G between ρ_S(N) and a(N)[16a], which is excellent for this case, because the experimental a(N) value for $H_4N_2^+$ is 11.5 G.[16b] It is seen in Figure 4 that syn bending is calculated by MNDO to raise a(N) considerably faster than anti bending. The ab initio values were calculated as the expectation value of the Fermi contact part of the spin Hamiltonian.[17] a(N) was calculated to be 18.936 and 23.93 G for planar $H_4N_2^+$ at the STO-3G and 6-31G UHF levels, respectively. Although the agreement with experiment is poor, the relative changes upon bending are reasonable. Both STO-3G and 6-31G calculations agree that a(N) increases more rapidly for syn bending than anti bending. The decrease in a(N) upon bending anti calculated by STO-3G is qualitatively unreasonable and may be due to the poor description of the 1s orbital on nitrogen; 6-31G calculates an increase in a(N) upon bending anti. These increases in a(N) upon bending are comparable to the changes obtained by MNDO and qualitatively agree with experimental data on $R_4N_2^+$.[2]

The behavior of the π,π^* energy gap as the nitrogens are bent is particularly interesting. Bending at nitrogen reduces the overlap between the nitrogen lone pair orbitals, and as shown in Figure 5, bending anti decreases it more rapidly than bending syn.[18]

(11) Hoffmann, R. *Acc. Chem. Res.* **1971**, *4*, 1.
(12) Nelsen, S. F.; Kessel, C. R.; Brien, D. J. *J. Am. Chem. Soc.* **1980**, *102*, 702.
(13) Bock, H.; Kalm, W.; Nöth, H.; Semkow, A. *J. Am. Chem. Soc.* **1980**, *102*, 442.
(14) Dewar, M. J. S.; Thiel, W. *J. Am. Chem. Soc.* **1977**, *99*, 4899, 4902. Program No. 353, Quantum Chemistry Program Exchange, Indiana University, Bloomington, IN.
(15) GAUSSIAN 77/UCL (written by DeFrees, D. J.; Levi, B. A.; Pollack, S. K.; Blurock, E. S.; Hehre, W. J.). We obtained it from Prof. G. M. Maggiora (University of Kansas).
(16) (a) Pople, J. A.; Beveridge, D. L.; Dobosh, P. A. *J. Am. Chem. Soc.* **1968**, *90*, 4201. (b) Adams, J. Q.; Thomas, J. R. *J. Chem. Phys.* **1963**, *39*, 1904.
(17) The form of the operation was taken from Chung: Chung, A. L. H. *J. Chem. Phys.* **1967**, *48*, 5532.
(18) (a) We note that Hoffmann stated[11] that lone-pair overlap in trans diimide is "probably" larger than that in cis diimide. We believe that trans/anti overlap is always smaller than cis/syn overlap at a given amount of bend, although it usually appears true that anti orbital, orbital interactions are larger than syn interactions. (b) We used lone-pair natural hybrid orbitals in the calculation of S, using the program BONDO, and the geometries of MNDO–UHF energy minimized $H_4N_2^+$. For a description of BONDO see Weinhold, F. A. University of Wisconsin Theoretical Chemistry Institute Technical Note 628G, Dec. 1979.

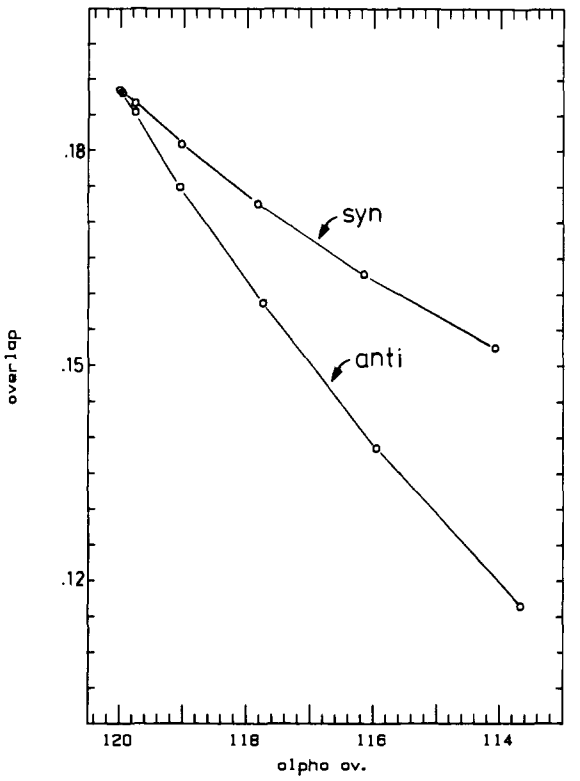

Figure 5. Plot of lone pair,lone pair hybrid AO overlap as a function of bending at nitrogen for MNDO energy-minimized $H_4N_2^+$.

From lone pair,lone pair overlap considerations, $\Delta E(\pi,\pi^*)$ should be larger for syn bending a given amount than for anti bending, and the difference should increase as the amount of bending increases. The opposite behavior is in fact calculated to occur. This indicates that the σ,π mixing shown in Figure 3 is large enough to overcome the direct overlap effect, which is in the opposite direction.

We have used two methods to calculate the π,π^* transition energies for hydrazine radical cation. Clark[19] pointed out to us the utility of the Koopmans' theorem "trick". The π,π^* Koopmans' energy gap given by an energy minimized UHF calculation for a doublet species like $H_4N_2^+$ is far from the π,π^* transition energy because the orbital occupancies are different, but to a good approximation, this energy gap is obtained correctly when the neutral species is calculated in the geometry of the radical cation, so that the orbital occupancies of π and π^* are the same. We will refer to this as the NCG (neutral in cation geometry) approximation for obtaining the π,π^* transition energy. The second method we have used is to calculate the energy of the vertical first excited state doublet species and subtract from it the energy of the ground state doublet species. The programs we have available require calculation of the excited doublet at the restricted Hartree–Fock level, so we used the energy of the ground-state doublet at the RHF level of calculation as well and will refer to π,π^* transition energy obtained in this manner as having used the RHF method. Comparison of the RHF and NCG methods for calculating λ_m are shown for STO-3G (Figure 6), 6-31G (Figure 7), and MNDO (Figure 8) calculations; in all three cases, the asterisks show the RHF and the circles the NCG results. We found the excellent agreement between these two methods of calculating λ_m surprising; for the ab initio methods, differences of under 3 nm in λ_m values are obtained at all amounts of bend. On the other hand, the λ_m values obtained at both ab initio levels appear to be rather smaller than the experimental value for $H_4N_2^+$. Pulse radiolysis measurements give an ϵ of 1500 at 225 nm.[20] Experimental problems precluded going to shorter wavelength to actually determine λ_m, but the observed ϵ values of 4500–2100 for anti bent $R_4N_2^+$ species $\mathbf{1}^+$–$\mathbf{3}^+$ (Table I) suggest that λ_m of $H_4N_2^+$ is below 225 nm, possibly near 200–210 nm. One would expect a shift to longer wavelength for λ_m of a radical cation in condensed phase compared

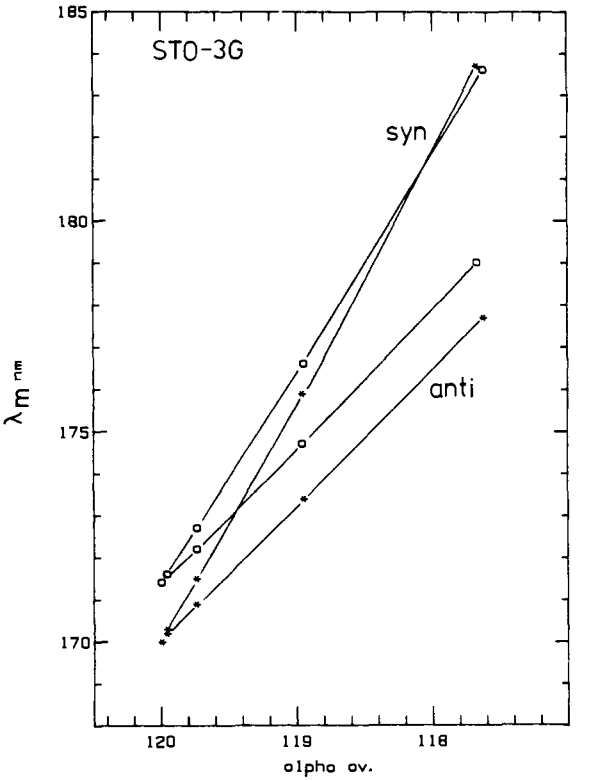

Figure 6. Plot of λ_m vs. α_{av} for $H_4N_2^+$ as calculated by STO-3G: (*) λ_m calculated by using the RHF method, (O) λ_m calculated by using the NCG method.

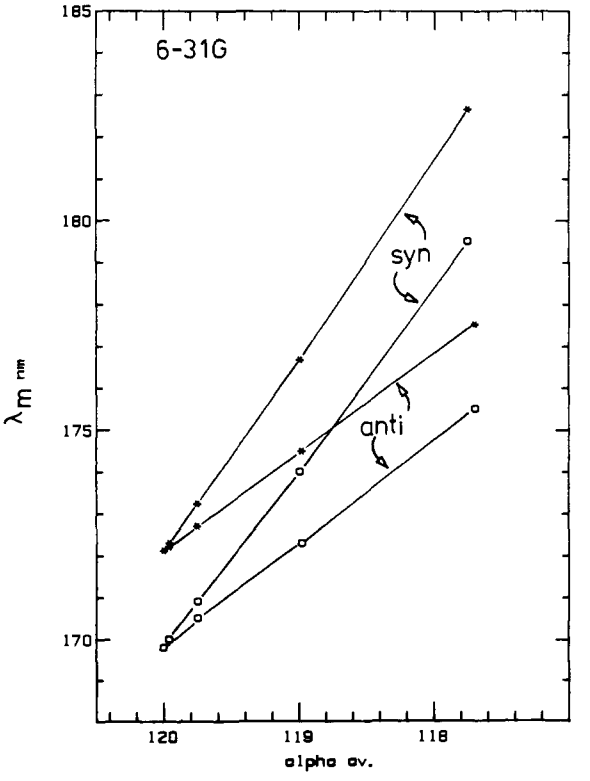

Figure 7. Plot of λ_m vs. α_{av} for $H_4N_2^+$ calculated by 6-31G: (*) λ_m calculated by using the RHF method, (O) λ_m calculated by using the NCG method.

(19) (a) Dr. T. Clark, University of Erlangen, private communication. A manuscript on its application to olefin radical cation electronic spectra is in preparation by Clark. (b) The NCG method is implicit in Figure 1 of ref 21b.

(20) Hayon, E.; Simic, M. *J. Am. Chem. Soc.* **1972**, *94*, 42.

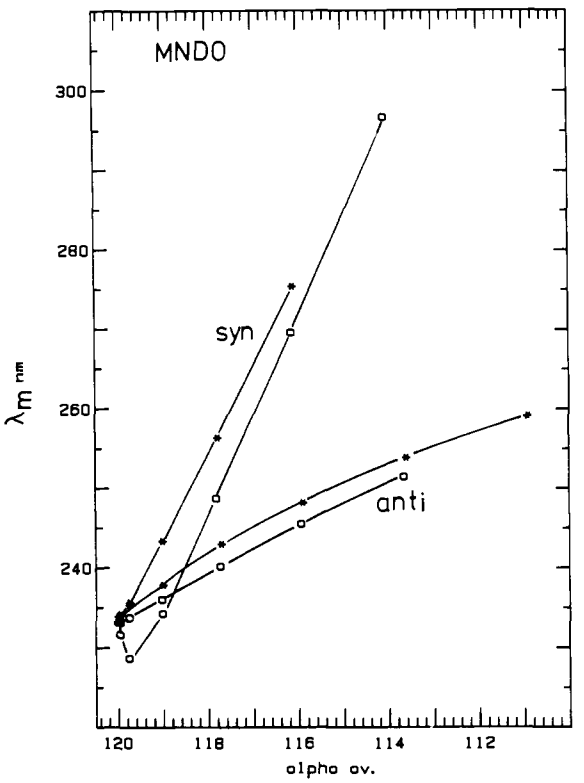

Figure 8. Plot of λ_m vs. α_{av} for $H_4N_2^+$ calculated by MNDO: (*) λ_m calculated by using the RHF method, (O) λ_m calculated by using the NCG method.

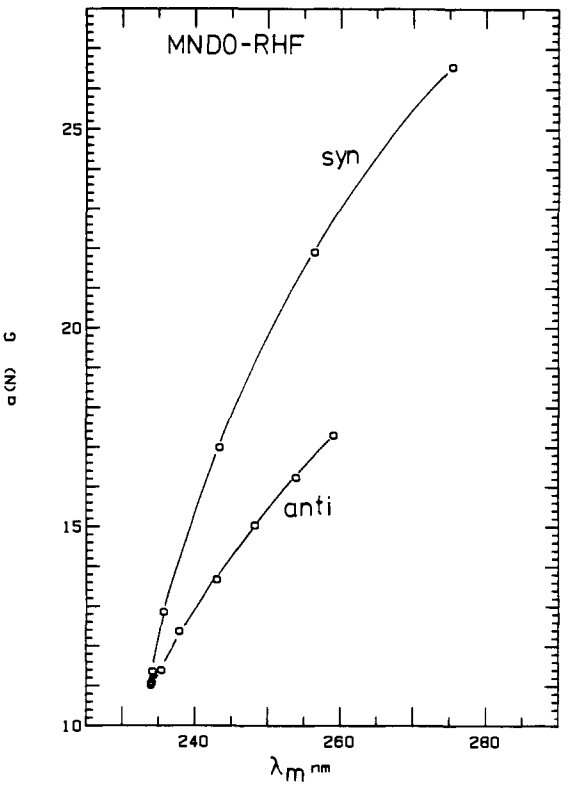

Figure 9. Plot of a(N) vs. λ_m for $H_4N_2^+$ calculated by using MNDO–RHF.

to gas phase (which is what calculations should give). Although absorption spectra of gas-phase radical cations are difficult to obtain experimentally because of concentration problems, they may be accurately estimated from the photoelectron spectra of compounds which do not change geometry much upon electron removal, and comparison of gas-phase UV data and condensed-phase UV absorption data has allowed examination of the size of the red shift.[21] It is found to be rather small, on the order of 0.03–0.09 eV for aromatic systems like naphthalene, and is smaller for polar matrices than for nonpolar ones. We would estimate that the closest analogy to what would be expected for a hydrazine radical cation would be 1,4-diazabicyclooctane (Dabco), where the red shift is larger, 0.51 eV. We would argue that there is enough geometry change in Dabco that part of this red shift may well be a geometry change effect, but we point out that a 0.5-eV red shift at 200 nm corresponds to a shift of λ_m of 15 nm. The MNDO λ_m value of about 233 nm for the planar species (Figure 8) is rather larger than the experimental value. The NCG approximation curve using MNDO for λ_m vs. α_{av} shows curious crossing of the syn and anti bending curves at small amounts of bending ($120 < \alpha_{av} < 118.7°$). Examination of the π and π^* energy levels shows that this crossing is entirely caused by the π^* energy level initially destabilizing as syn bending occurs. Such crossing does not occur for MNDO with use of the RHF method for calculating λ_m or either method with ab initio calculations, so we presume it is an artifact.

Because α_{av} is never known for hydrazine radical cations in solution, we give a plot of experimentally measurable quantities, a(N) vs. λ_m, as Figures 9 and 10. The RHF method has been used for calculation of λ_m in both cases. The 6-31G a(N) values (Figure 10) used the Fermi contact expectation values. Figures 9 and 10 show separate branches for *syn* and *anti* bending, caused by the strong σ,π mixing which occurs upon bending at nitrogen.

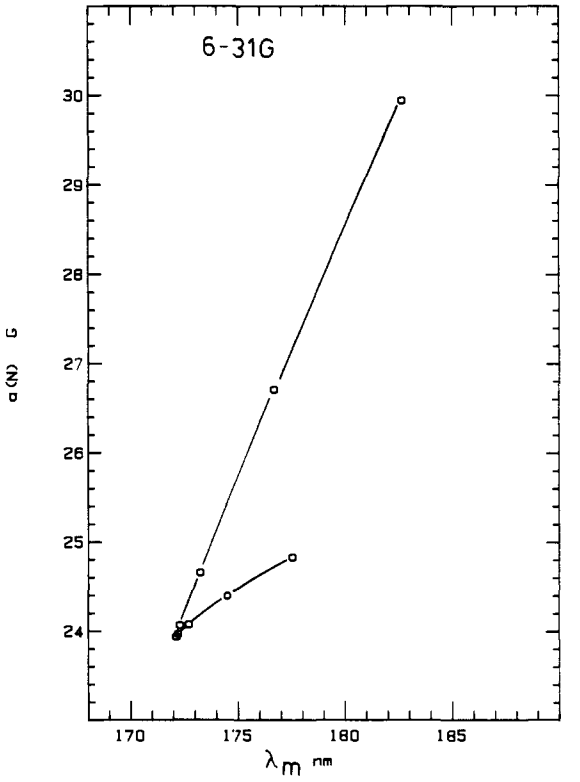

Figure 10. Plot of a(N) vs. λ_m for $H_4N_2^+$ calculated by using 6-31G.

Discussion: Comparison of Experimental $R_4N_2^+$ and Calculated $H_4N_2^+$ Data

Comparing the a(N) vs. λ_m experimental plot of Figure 1 with the calculated plots of Figures 9 and 10 shows a rather similar rapid rise for the syn bent structures, but the experimental anti branch is far flatter in the experimental data of Figure 1 than in the calculated data. In fact, it appears that measurement of a(N) and λ_m makes a cleaner distinction between syn and anti bent $R_4N_2^+$ than calculations on $H_4N_2^+$ suggest would be the case.

(21) (a) Shida, T.; Nosaka, Y.; Kato, T. *J. Chem. Phys.* **1978**, *82*, 695. (b) Haselbach, E.; Bally, T.; Gschwind, R.; Klemm, U.; Layiova, Z. *Chimia* **1979**, *33*, 405. (c) Haselbach, E.; Klem, V.; Buser, V.; Gschwind, R.; Jurgen, H.; Kloster-Jensen, E.; Maier, J. P.; Marthaler, O.; Christen, H.; Baertschi, P. *Helv. Chim. Acta* **1981**, *65*, 823. (d) Shida, T.; Haseblach, E.; Bally, T. *Acc. Chem. Rev.* **1984**, *17*, 180.

Table II. Twisting Anti Bent $H_4N_2^+$, MNDO Calculations

ω_A	ΔH_f, kcal/mol	Δa(N),[b] G	$\Delta\lambda_m$,[c] nm
180	213.3	[0]	[0]
170	213.8	0.07	6.5
160	215.0	0.29	25.4
150	217.2	0.62	56.7
140	220.2	1.08	106.3
130	224.2	1.59	181.6
120	229.1	2.09	315.1

[a] Lone pair,lone pair dihedral angle (degrees). [b] a(N) for $\theta = 180° - a$(N) for θ; a(N) decreases as twisting increases. [c] $\lambda_m(\theta) - \lambda_m(\theta = 180°)$; λ_m increases as twisting increases. Calculated by the NCG procedure.

The differences in spectral data observed for what must be very small differences in the geometry at nitrogen for syn and anti bent $R_4N_2^+$ are a surprisingly large result of the difference in σ,π mixing symmetry for syn and anti bending.

Several factors must be considered for a meaningful comparison of the differences between Figures 1 and 9/10. First, the sources of the bending which cause a dispersion of points in each figure are different. The calculated plots achieve bending by arbitrarily fixing an HN,NH dihedral angle and minimizing the energy of $H_4N_2^+$ otherwise. For the real compounds of Figure 1, the range of bending is imposed by the shape of the attached alkyl groups, so that interactions between these alkyl groups will also influence the geometry, and hence the spectral parameters, in a way that is entirely missing from Figure 9/10. The clearest example of such alkyl,alkyl interaction involves the red shift of acyclic examples **11** and **12**, which have one and two *tert*-butyl substituents, respectively. It is clear that *N,N'-tert*-butyl,methyl interaction in these species would be relieved by twisting about the NN bond, and it has been proposed before that this occurs.[2,13] MNDO calculations on anti $H_4N_2^+$ as a function of twisting about the NN bond (using the NCG approximation) are summarized in Table II, where in agreement with INDO calculations[13] a(N) is calculated to decrease and λ_m to increase. We have not measured the a(N) values for **11** (there will be two, and they are both close to the a(Me) values, leading to a complex spectrum), but a(N) for **12** is significantly smaller than that for most $R_4N_2^+$.[2] From the calculations of Table II, the 42–45-nm red shift of $\mathbf{11}^+$ (compared to that of $\mathbf{9}^+$ and $\mathbf{10}^+$) might correspond to a 27° twist about the NN bond, and the 125–128-nm red shift of $\mathbf{12}^+$ and its 1.2 G decrease in a(N) might correspond to a 43° twist. It must be emphasized, though, that steric interactions should increase the NN bond length as well as lead to twisting. Since an increase in NN bonding length would also cause a red shift of λ_m, the 27° and 43° twist values derived from Table II are doubtless too high. We have no way at present of estimating how much too high they might be.

In a similar vein, the α-tertiary centers of $\mathbf{2}^+$ will make this hydrazine cation harder to bend at nitrogen than less highly substituted examples, which would lead to a blue shift in λ_m. On the other hand, the tertiary carbon, secondary carbon interactions in $\mathbf{2}^+$ are expected to cause an increase in NN bond length, which will lead to a red shift. Experimentally, λ_m for $\mathbf{2}^+$ and $Me_4N_2^+$ ($\mathbf{8}^+$) are the same.

One trend worth noting is the blue shift of syn hydrazine cations compared to anti ones for examples which are not bent very much. The syn hydrazines of Table I only have larger λ_m than the anti compounds when a(N) is substantially larger. We suggest that this might also be an NN bond-length effect. The syn compounds are all NN′ cycloalkyl, so that increasing the NN bond length is opposed by the need to expand ring bond angles. This effect is not present for the anti bent compounds, which might lead to a longer NN bond length and hence a red shift for all of the anti bent compounds relative to the syn bent compounds. Structural data on syn bent compounds, now totally lacking, will be required to test this hypothesis.

Accurate calibration of the amount of bending represented by the various points in Figure 1 is clearly complex. Since defining the structure requires at least locating the two nitrogens and four α carbons in space, the two numbers a(N) and λ_m clearly cannot really define the geometry. $R_4N_2^+$ is flexible enough that a(N) is a time average over a range of bending geometries, and the size of the range will depend upon compound. Our best case for knowing α_{av} demonstrates that even having a crystal structure does not solve the problem of estimating the amount of bending. Crystalline $\mathbf{3}^+$ has $\alpha_{av} = 115.6°$, but its ENDOR spectrum shows it cannot be this bent in solution. Use of the bridgehead splitting to estimate the average amount of bend is solution gives a β(NN) value of 18°, leading to an α_{av} estimate of about 118.7°.[8]

Table III. Geometry-Optimized $H_4N_2^+$

	MNDO–UHF	STO-3G	6-31G
β(NN), deg	25.4 (anti)	26.7 (anti)	0.0 (planar)
∠NNH, deg	118.60	117.26	119.92
α_{av}, deg	117.7	117.6	120.0
d(NN), Å	1.2955	1.3458	1.2982
d(NH), Å	1.0214	1.0408	0.9992

Conclusion

Mixing of σ and π orbitals upon bending at nitrogen in $R_4N_2^+$ leads to unusually large sensitivity of a(N) and λ_m to the R groups. The difference in the symmetry of the mixing for syn and anti bending causes a(N) to increase much faster with syn bending then with anti bending and causes syn and anti compounds to appear in separate distributions on an a(N) vs. λ_m plot. It appears to be feasible to tell whether $R_4N_2^+$ examples are syn or anti bent and rank examples in terms of average amounts of bending at nitrogen by using a(N) and λ_m values. The twisting and lengthing of the NN bond which accompanies *tert*-butyl substitution is quite noticeable, giving about 45- and 125-nm red shifts for replacement of one and two primary or secondary alkyl groups by *tert*-butyl groups in acyclic $R_4N_2^+$ examples.

Experimental Section

Compounds. Preparations have been reported for **1**,[22] **2**,[6] **3**,[7,8] **6**, and **8–15**.[23] **4**, **5**, and **7** were made by Diels–Alder addition of the appropriate diene to protonated bicyclic azo compounds followed by deprotonation and reduction. The characterization and preparation of these compounds will be reported separately.

UV spectra were recorded on a Cary 118 instrument. Isolated radical cation salts were simply dissolved in acetonitrile. Solutions of the cation nitrates of **5–8** were prepared by oxidizing a 1 mM solution with silver nitrate, centrifuging off the silver sludge, and recording the UV spectrum. For **9–15**, a flow cell modified from the design of Clark and Evans[24] was employed. The porous bed working electrode was constructed of reticulated vitreous carbon (100 pores per in., Chemotronics International, Inc., Ann Arbor, MI), force fit in 6-mm OD "thirsty" glass tubing (Corning 7930). Solution was forced through this flow cell and into a flow UV cell in the Cary 118 spectrometer by using a syringe pump (flow rate about 0.5–1.5 mL/min). The working electrode potential was maintained by using a PAR 132 electrochemically apparatus. Experiments using tris(*p*-bromophenyl)amine showed that radical cation production efficiency was over 90%, and the minimum ϵ values of Table I assume 100% efficiency.

ESR Spectra were recorded on a Varian E-15 spectrometer, as previously described.[2,3]

MO Calculations on $H_4N_2^+$. Bending in syn and anti directions was enforced by setting the angle between the NH bonds and dummy atom positions in space. MNDO-UHF energy minimization (using the default minimization criteria of the program) was performed at each degree of bend with use of Dewar's program.[14] The lone pair,lone pair overlap was calculated for the MNDO geometry by using the program BONDO.[18b] STO-3G and 6-31G calculations used GAUSSIAN 77.[15] Geometries were optimized to 0.001 Å in bond lengths and 0.01° in bond angles. The excited doublet state calculations were performed with the program MELD,[25] which required using a restricted open-shell Hartree–Fock procedure, which is slightly inconsistent with the UHF procedure used to

(22) Nelsen, S. F.; Hollinsed, W. C.; Kessel, C. R.; Calabrese, J. C. *J. Am. Chem. Soc.* **1978**, *100*, 7876.
(23) Nelsen, S. F.; Peacock, V. E.; Weisman, G. R. *J. Am. Chem. Soc.* **1976**, *98*, 5269.
(24) Clark, B. R.; Evans, D. H. *J. Electroanal. Chem.* **1976**, *69*, 181.
(25) MELD was kindly provided by E. R. Davidson at the University of Washington.

minimize the geometries. Table III contains some information on the energy-minimized $H_4N_2^+$ geometries obtained in this work. Complete information on the calculated energies, geometries, and spin densities is available by writing the authors.

Acknowledgment. We thank the National Science Foundation and the National Institutes of Health for partial financial support of this work under grants CHE-8026111 and GM 29549, respectively, and the NSF for a Fellowship to J.E.C. We thank Dan Kapp for assistance in construction of the flow electrochemical cell.

Registry No. 1, 62781-95-7; 2, 82666-13-5; 3, 86711-99-1; 4, 90046-51-8; 5, 93601-00-4; 6, 60512-67-6; 7, 93473-65-5; 8, 34504-32-0; 9, 93473-66-6; 10, 93473-67-7; 11, 93473-68-8; 12, 93473-69-9; 13, 42843-04-9; 14, 93601-01-5; 15, 93473-70-2; $H_4N_2^+$, 34504-42-2.

Theoretical Studies of [1,*n*]-Sigmatropic Rearrangements Involving Hydrogen Transfer in Simple Methyl-Substituted Conjugated Polyenes

B. Andes Hess, Jr.,* L. J. Schaad,* and J. Pancíř†

Contribution from the Department of Chemistry, Vanderbilt University, Nashville, Tennessee 37235. *Received April 3, 1984*

Abstract: Transition structures for the [1,*n*]-sigmatropic hydrogen shift in 1-propene (n = 3), (*Z*)-1,3-pentadiene (n = 5), and (3*Z*,5*Z*)-1,3,5-heptatriene (n = 7) have been studied by using ab initio SCF and correlated wave functions with several basis sets from STO-2G to 6-31G*. Antarafacial transition structures were found for propene and heptatriene and suprafacial for pentadiene, as predicted by the Woodward–Hoffmann rules. Activation energies were also obtained and were found to decrease significantly from the [1,3]- to the [1,5]- to the [1,7]-hydrogen shift in agreement with earlier experimental results. The deuterium isotope effect for the [1,5] shift has been computed ab initio and found in poor agreement with experiment.

Sigmatropic rearrangements that involve hydrogen transfer have been of considerable theoretical[1-5] and experimental[6] interest since the stereochemistry of their transition structures was predicted by Woodward and Hoffmann.[7] They stated that the [1,3]-, [1,7]-, ··· hydrogen migrations would have transition structures corresponding to an antarafacial hydrogen migration while the [1,5]-, [1,9]-, ··· hydrogen migration would have transition structures with suprafacial stereochemistry. Quite recently Dewar has questioned the synchronous nature of many concerted reactions.[8] However, he noted that [1,*n*]-sigmatropic rearrangements that involve hydrogen transfer are likely to be an exception to his rule that "synchronous multibond mechanisms are normally prohibited" and therefore are likely to have symmetric transition structures.

We have undertaken a systematic theoretical study of the [1,3]-, [1,5]-,[9] and [1,7]-sigmatropic hydrogen-transfer rearrangements in the corresponding methyl-conjugated linear polyenes (**1–3**). Both transition structures and activation energies have been examined.

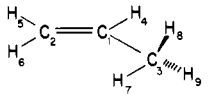

1

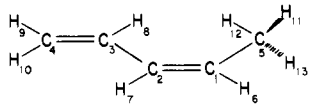

2

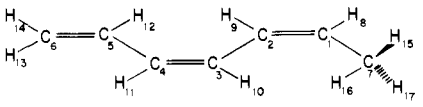

3

Results

All computations were done on Vanderbilt University's DEC-10 and DEC-20 computers with use of Pople's GAUSSIAN 80 program[10] for the SCF runs and an MP2 program[11] written to take advantage of molecular symmetry for the correlation energy calculations.

Table I. Optimized Geometry of Propene (**1**)[a,b]

coordinate	3-21G	6-31G	6-31G*
C_1–C_2	1.316	1.324	1.318
C_1–C_3	1.510	1.502	1.503
C_1–H_4	1.076	1.074	1.079
C_2–H_5	1.073	1.074	1.076
C_2–H_6	1.075	1.075	1.077
C_3–H_7	1.083	1.083	1.084
C_3–H_8	1.086	1.086	1.087
C_3–H_9	1.086	1.086	1.087
$\angle C_2C_1C_3$	124.7	125.1	125.1
$\angle C_1C_2H_5$	121.9	121.8	121.6
$\angle C_1C_2H_6$	121.8	121.9	121.9
$\angle C_2C_1H_4$	119.6	119.1	118.9
$\angle C_1C_3H_7$	111.1	111.4	111.4
$\angle C_1C_3H_8$	110.6	111.0	110.9
$\angle C_1C_3H_9$	110.6	111.0	110.9
$\angle C_2C_1C_3H_7$	180.0	180.0	180.0
$\angle C_2C_1C_3H_8$	120.5	120.5	120.6
$\angle C_2C_1C_3H_9$	120.5	120.5	120.6

[a] Bond distances in angstroms and angles in degrees. [b] C_s symmetry assumed.

† Permanent address: J. Heyrovský Institute of Physical and Electrochemistry, Czechoslovak Academy of Sciences, Prague.

(1) Bingham, R. C.; Dewar, M. J. S. *J. Am. Chem. Soc.* **1972**, *94*, 9107.
(2) Castenmiller, W. A. M.; Buck, H. M. *Tetrahedron* **1979**, *35*, 397.
(3) Bouma, W. J.; Vincent, M. A.; Radom, L. *Int. J. Quantum Chem.* **1978**, *14*, 767.
(4) Rodwell, W. R.; Bouma, W. J.; Radom, L. *Int. J. Quantum Chem.* **1980**, *18*, 107.
(5) Bernardi, F.; Robb, M. A.; Schlegel, H. B.; Tonachini, G. *J. Am. Chem. Soc.* **1984**, *106*, 1198.
(6) Reviews of experimental results: (a) Gajewski, J. J. In "Mechanisms of Molecular Rearrangements"; Thyagarajan, B. S., Ed.; Wiley-Interscience: New York, 1971; Vol. 4, pp 1–53. (b) Gajewski, J. J. "Hydrocarbon Thermal Isomerizations"; Academic Press: New York, 1981. (c) Spangler, C. W. *Chem. Rev.* **1976**, *76*, 187. (d) Gilchrist, T. L.; Storr, R. C. "Organic Reactions and Orbital Symmetry"; Cambridge University Press: London, 1972. (e) Gill, G. B. *Q. Rev. Chem. Soc.* **1968**, *22*, 338.
(7) Woodward, R. B.; Hoffmann, R. "The Conservation of Orbital Symmetry"; Academic Press: New York, 1970.
(8) Dewar, M. J. S. *J. Am. Chem. Soc.* **1984**, *106*, 209.

0002-7863/85/1507-0149$01.50/0